CHINESE OPTICS LETTERS

Vol. 19, No. 11 | November 2021

Vector dynamics of ultrafast cylindrical vector beams in a mode-locked fiber laser

Jiazhu Wang (王家柱), Liang Jin (金 亮)*, Shangzhi Xie (谢尚之), Renyan Wang (王仁严), He Zhang (张 贺), Yingtian Xu (徐英添), Xin Zhao (赵 鑫), Yan Li (李 岩), and Xiaohui Ma (马晓辉)

National Key Laboratory on High-power Semiconductor Lasers, Changchun University of Science and Technology, Changchun 130022, China

*Corresponding author: jinliang@cust.edu.cn

Received July 23, 2021 | Accepted September 29, 2021 | Posted Online October 22, 2021

The vector dynamics of solitons are crucial but easily neglected for realizing vortex solitons. In this Letter, we investigate the effect of vector dynamics on cylindrical vector beams (CVBs) implementation and propose a novel technical method to realize femtosecond CVBs based on vector-locked solitons, which are presented as group-velocity-locked vector solitons (GVLVSs) in the experiment. The outstanding vector properties of GVLVSs not only greatly improve the efficiency of solitons converted into CVBs and output power of CVBs (2.4 times and 4.1 times that of scalar solitons and vector change periodical solitons, with the purity of 97.2%), but also relax the obstacle of ultrafast CVBs from the fundamental frequency to the harmonic regime (up to 198 MHz) for the first time, to the best of our knowledge. This is the highest repetition rate reported for ultrafast CVBs based on passive mode-locking. The investigation of the influence of solitons vector dynamics evolution on the realization of CVBs provides guidance for the excellent performance of ultrafast CVBs.

Keywords: cylindrical vector beam; ultrafast optical switch; laser mode-locking.

DOI: 10.3788/COL202119.111903

1. Introduction

Cylindrical vector beams (CVBs) are optical beams that carry polarization singularities. Due to the unique polarization and amplitude characteristics of the optical fields of CVBs, many applications have been explored in the field of optical communication[1], surface plasmon excitation[2], optical trapping[3], etc. Furthermore, it is worth noting that the ultrafast CVBs pulse in a picosecond or femtosecond laser expands various new applications, such as in nonlinear frequency conversion[4], super-resolution microscopes[5], and material processing [6].

Ultrafast CVBs are generally obtained by mode excitation and selection of solitons from the mode-locked laser platform, where the soliton presented in the vector or scalar state[7–12]. Therefore, the inherent properties of solitons and mode control of solitons are crucial to the realization of ultrafast CVBs. Compared with solid-state lasers, the advantages of compactness, high beam quality, and stability of the all-fiber laser are more suitable for the platform of ultrafast CVBs[13–15]. Moreover, it is easy to generate CVBs because of the mode group in fiber, which includes TE_{01} (azimuthally polarized), TM_{01} (radially polarized), and HE_{21} (even and odd) vector modes. Thus, ultrafast LP_{11} can be obtained by exciting the LP_{11} mode and selecting TE_{01} and TM_{01} of the four vector modes of the LP_{11} mode.

In recent years, researches on ultrafast CVBs have focused on how to excite and select high-order modes to improve the conversion efficiency of LP_{01} to LP_{11} or the purity of ultrafast CVBs. In this context, the offset coupling spot (OSS), fiber grating, and mode selective coupler (MSC) have been employed to obtain ultrafast CVBs[16–19]. However, intrinsic insertion loss of OSS limits the conversion efficiency, and the relatively narrow spectral bandwidth and complex manufacturing process of MSC restrict the bandwidth of output beams. Compared to the other techniques, long-period fiber grating (LPFG) mode converters have the advantages of smaller size, lower loss, and design flexibility. As the latest progress, the ultrafast CVBs based on metasurfaces are becoming a new research hotspot[20–23]. With the deepening of research, the technology of solitons converting to CVBs is emerging and more and more advanced. In addition to using few-mode fiber gratings to excite and select higher-order modes, this article focuses on the effect of soliton vector characteristics on the conversion efficiency and purity of CVB, which is rarely mentioned in previous studies.

However, CVBs, as vector modes, are sensitive to the vector properties of solitons, but the influence of soliton vector dynamics on the realization of ultrafast CVBs has attracted little attention in previous research. In this Letter, we explore the role of soliton vector properties in realizing ultrafast CVBs and pay attention to the conversion efficiency of solitons to CVBs, rather than that of LP_{01} to LP_{11}. In the experiment, we innovatively demonstrate ultrafast CVBs based on vector-locked solitons

(group-velocity-locked vector solitons, GVLVSs) fiber laser platform. Compared with the ultrafast CVBs based on vector change periodic solitons and scalar solitons, the high polarization stability of vector-locked solitons not only greatly improves the efficiency of solitons converting into ultrafast CVBs, but also extends the ultrafast CVBs operation from the fundamental frequency to the harmonic regime for the first time, to the best of our knowledge. The output power and conversion efficiency of ultrafast CVBs based on vector-locked solitons are more than 2.4 times that based on scalar solitons and 4.1 times that based on vector change periodic solitons. Moreover, the superior vector stability of vector-locked solitons guarantees ultrafast CVBs operation at the repetition rate from 25 MHz to 198 MHz, with the pulse of ~856 fs.

2. Experiment Section

The configuration of the proposed all-fiber passively mode-locked GVLVSs laser setup is illustrated in Fig. 1(a). A 976 nm laser diode (LD) pumps a 35 cm long erbium-doped fiber (EDF) (Er80-8/125, Liekki) by a wavelength division multiplexer (WDM). A graded-index multimode fiber (GIMF) is inserted into the ring cavity and combined with the single fiber to form a single-mode fiber–graded-index multimode fiber–single-mode fiber (SMS) ultrafast switch. The set-up includes a polarization-independent isolator to ensure unidirectional propagation in the cavity, and a polarization controller (PC) to continuously adjust the in-cavity birefringence. A 90:10 coupler is utilized to extract the laser pulses through the 10% port. The output soliton train can be polarization-resolved along two birefringence axes with a polarization beam splitter (PBS) and PC2 external to the cavity.

Self-started mode-locking can be easily obtained as the lasing threshold is reached with the fundamental repetition rate

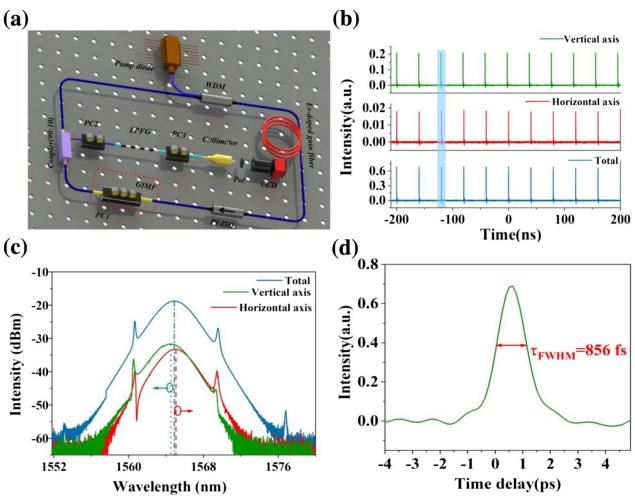

Fig. 1. (a) Experimental configuration of all-fiber GVLVSs fiber laser; (b) oscilloscope traces of these GVLVSs along the two orthogonal polarization axes; (c) polarization-resolved spectrum of GVLVSs; (d) pulse duration of GVLVSs.

of 25 MHz. Figure 1(b) depicts the oscilloscope trace after the polarization-resolved measurement. The pulse intensity of the two orthogonally polarized solitons (red and blue pulse trains) is uniform. Moreover, the central wavelengths of the vertical and horizontal components after being polarization-resolved are located on both sides of the total spectrum, which is a typical feature of the GVLVSs spectrum[24]. The main components of the spectrum are at wavelengths near 1564.72 nm, with the 3 dB spectral bandwidth as 3.38 nm, as shown in Fig. 1(c). The time and frequency domain characteristics of solitons indicate that they are GVLVSs. Figure 1(d) presents the pulse duration of GVLVSs, which is estimated to be 856 fs at the fundamental repetition rate, and it is fixed in and fitted to the hyperbolic secant pulse profile. The corresponding time-bandwidth product can be calculated as 0.346, which indicated that the output pulse almost reaches the theoretical limit.

By increasing the pump power above 35 mW, noisy pulsations are observed, corresponding to unstable multipulse mode-locking states. Upon increasing the pump power to 69 mW, stable harmonic mode-locking (HML) can be obtained, and the repetition rate reaches 75 MHz, corresponding to the third harmonic order. Figure 2 shows the oscilloscope traces of the typical mode-locked and HML operation evaluation at different pump powers. With proper adjustment of PC1, multiple pulses from the third up to the eighth HML are generated within the laser round trip at the pump power from 35 mW to 130 mW, corresponding to 75 MHz, 175 MHz, and 198 MHz, as shown in Figs. 2(b)–2(d). The RF spectrum of GVLVSs from fundamental to HML regimes is shown in Fig. 2(e)–2(h). The RF spectrum at the fundamental repetition rate is 25 MHz at 35 mW, and the signal-to-noise ratio (SNR) exceeds 44 dB. With the maximum pump power, the SNR for the eighth harmonic solitons is 49.1 dB. In the whole process, there is no satellite peak emerging in the RF spectrum, which indicates that there is no vector resonance modulation instability (VRMI) in the harmonic mode-locked state.

In order to obtain the ultrafast CVBs, an LPFG, inscribed on a graded-index two-mode fiber (FM GI-2, YOFC) by a CO_2-laser source (CO2-H10, Han's Laser), is connected to the output port and demonstrated as a mode converter. The intensity profiles of the radially and azimuthally polarized beams are captured by the CCD camera (CinCam CMOS-1201). The transmission spectrum of the TM-LPFG is shown in the red curve in Fig. 3(a). The transmission spectrum bandwidth of the LPFG is 5 nm, from 1563 nm to 1568 nm, which covers the central wavelength of the vector mode-locked fiber laser. The surface morphology of TM-LPFG is shown in Fig. 3(b), the period is 700 μm, and the illustration is the details of the TM-LPFG. In the experiment, the GVLVSs based on SMS can operate at both radially and azimuthally polarized modes throughout the fundamental repetition rate and HML, and the doughnut shape intensity profiles are shown in Figs. 4(a1) and 4(f1), respectively. The ultrafast CVBs emission has high mode purity that is calculated to be 97.2% by calculating the percentage bending loss[25]. In order to estimate the polarization states of the output, a linear polarizer is sandwiched between the output port and CCD. After the output

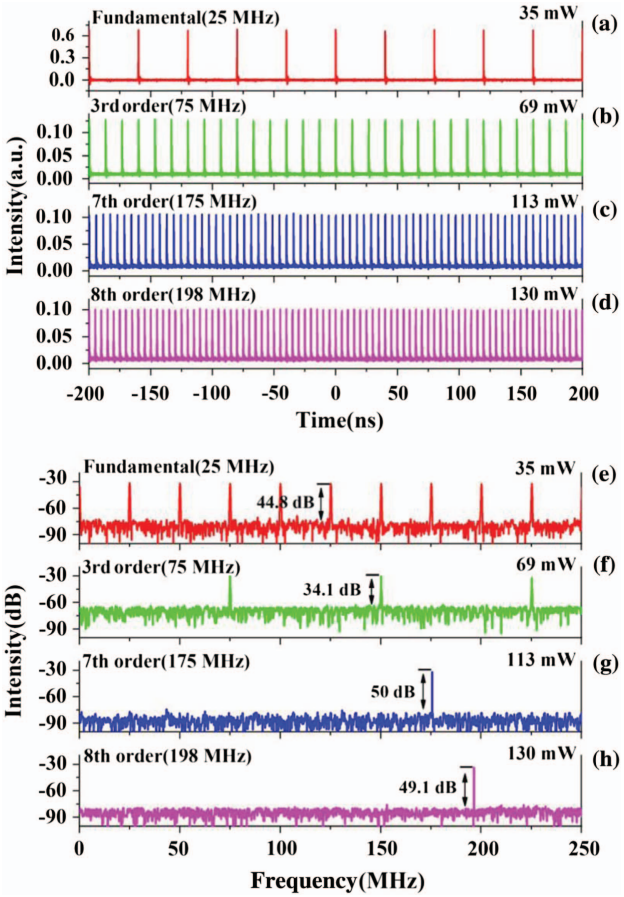

Fig. 2. (a)–(d) Oscilloscope trace and (e)–(h) RF spectrum of the output pulses at different pump power.

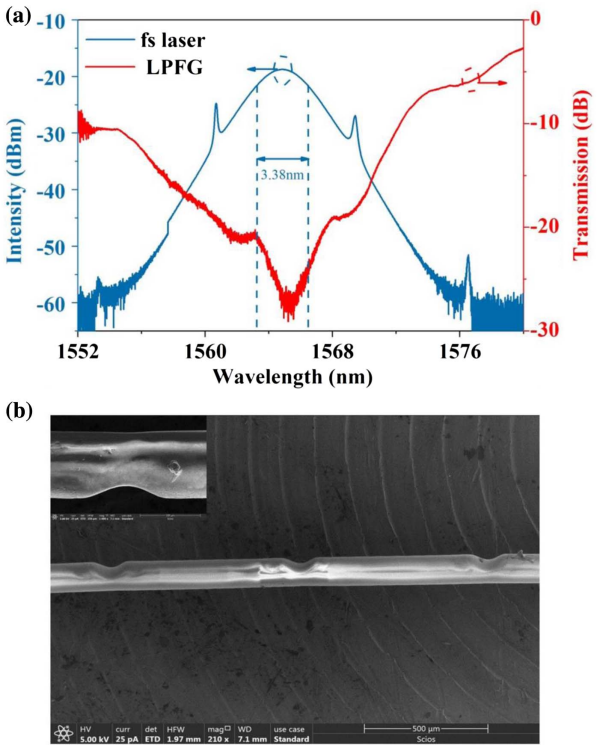

Fig. 3. (a) Transmission spectrum of LP_{01} mode of the TM-LPFG; (b) the surface morphology of TM-LPFG (inset: enlarged part).

beam passes through the linear polarizer, the two-lobe profiles are obtained by rotating the polarizer, and the transmission orientations are represented by the four white arrows, as shown in Figs. 4(b1)–4(e1) and 4(g1)–4(j1). Moreover, the stable ultrafast CVBs can be obtained in the 3rd, 7th, and 8th HML states by adjusting PC2 and PC3 carefully. In order to clarify the influence of soliton vector properties on ultrafast CVBs generation, we introduce the vector solitons based on carbon nanotube (CNT) mode-locking and the scalar solitons based on nonlinear polarization rotation (NPR) mode-locking in the experiment. To make the experimental results more convincing, other conditions in Fig. 1(a) remain unchanged except for mode-locking methods. The doughnut shape intensity profiles obtained by CNT and NPR-based mode-locking are shown in Figs. 4(a2)–4(j2) and 4(a3)–4(j3). The irregular speckles appearing in the intensity profiles indicate the existence of mode crosstalk in CVBs based on CNT and NPR mode-locking, and the speckles based on scalar solitons (NPR mode-locking) are more serious than those based on vector solitons (CNT and SMS mode-locking). The output light based on vector-locked solitons has the best density and the fewest stray speckles, which comes from the stable polarization state in the cavity. When the polarization state of the soliton changes, the mode crosstalk between different modes becomes extremely serious. Apart from that, when such beams pass through the long-period grating (LPG), the excited high-order modes are in an unstable state, and part of the light will be scattered into the cladding and will excite the cladding modes causing mode crosstalk, which is the source of CVB stray light. Figure 5 shows the output power of ultrafast CVBs depending on the SMS, CNT, and NPR mode-locking. The output power of ultrafast CVBs and the conversion efficiency of GVLVSs to ultrafast CVBs are 2.4 times that based on NPR mode-locking and 4.1 times that based on CNT mode-locking. Therefore, the vector properties of the soliton determine the output characteristics of ultrafast CVBs.

Since the CVBs are vector modes, the polarization dynamics of solitons should be investigated to explain the role of solitons vector properties in the process of ultrafast CVBs formation. We used a polarimeter (PAX1000IR2/M, Thorlabs) to record the state of polarization (SOP) based on SMS, CNT, and NPR mode-locking operation. The polarization evolution for fundamental and HML regimes based on SMS mode-locking is shown in Figs. 6(a) and 6(b). The GVLVSs can be observed on the surface of a Poincaré sphere at the fundamental frequency and HML regime, as shown in Fig. 6(a). GVLVSs based on SMS mode-locking are associated with a fixed points polarization attractor on a Poincaré sphere. The observed phase difference of GVLVSs indicates that GVLVSs are polarization-fixed left-handed and right-handed vector-locked solitons. The degree of polarization (DOP) corresponding to the fundamental repetition rate and harmonic regime is higher than 75% and

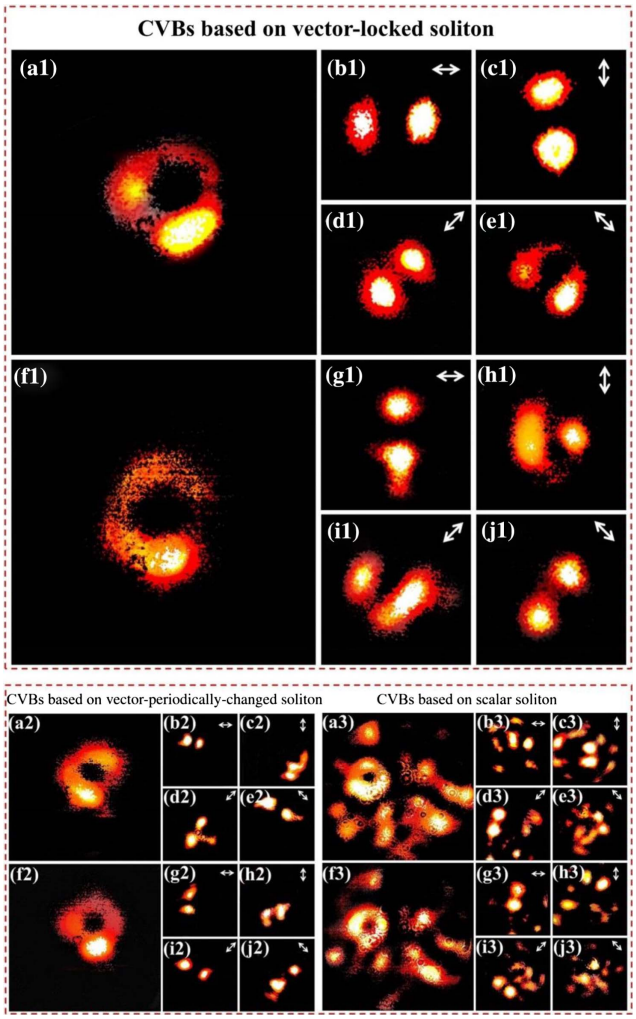

Fig. 4. Intensity profiles of ultrafast CVBs based on vector-locked and non-vector-locked solitons. (a) and (f) are radially and azimuthally polarization beams without a polarizer; (b)–(e) and (g)–(j) show the profiles of the output beam after passing through a linear polarizer. Arrow indicates the orientation of the linear polarizer.

achieves the maximum value of ~93% at the fundamental repetition rate, as shown in Fig. 6(b), where the DOP and phase difference of vector-locked solitons are fixed as constants. Figures 6(c) and 6(d) are the measured polarization dynamic states based on CNT mode-locking. Figure 6(c) shows that the polarization attractor generated by the rapid jump of phase difference is a line on the Poincaré sphere. The trajectory of rapid oscillation can be seen from the evolution of phase difference shown in Fig. 6(d). The oscillation trajectory in the fixed orientation indicates that the solitons have vector properties and change periodically. Therefore, the solitons obtained by CNT mode-locking are vector-periodically-changed solitons. Figures 6(e) and 6(f) are the measured polarization dynamic states based on NPR mode-locking. The polarization attractor on the Poincaré sphere contains a circular region close to the pole of the Poincaré sphere, and the randomness of oscillation orientation of the polarization attractor indicates that

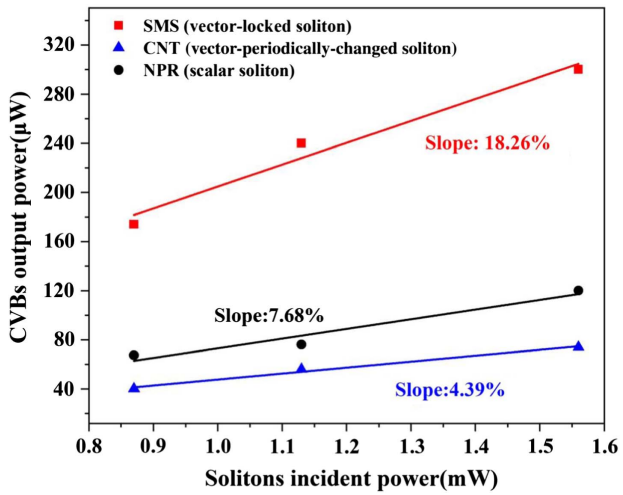

Fig. 5. Output power of ultrafast CVBs depends on the incident power of vector and non-vector-locked solitons.

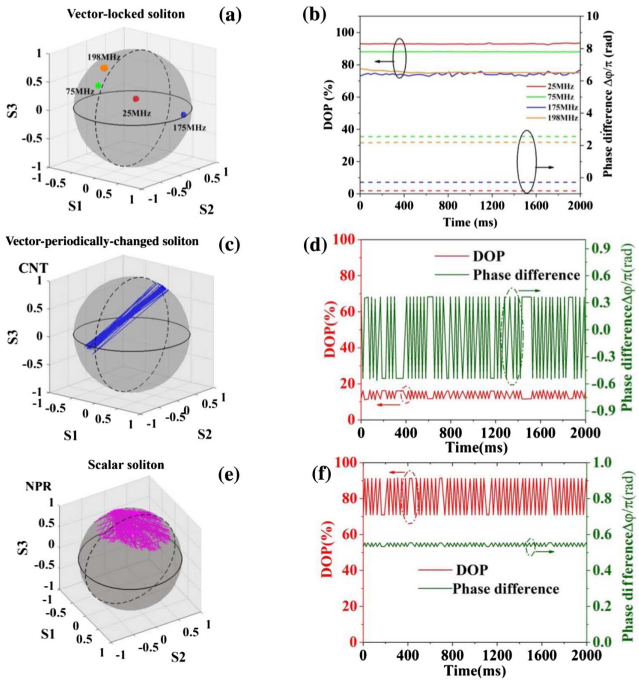

Fig. 6. Time evolution of solitons based on SMS, CNT, and NPR mode-locking in terms of (a), (c), (e) Stokes parameters at the Poincaré sphere and (b), (d), (f) intensities of orthogonally polarized modes.

the solitons based on NPR mode-locking are scalar solitons. Therefore, the vector properties of solitons determine the conversion efficiency of solitons into ultrafast CVBs and the output characteristics of ultrafast CVBs.

To explain the relationship between soliton vector properties and CVBs, we need to establish the vector distribution of CVBs. Figure 7 illustrates the polarization and intensity profiles of CVBs. The expression of CVBs in cylindrical coordinates is as follows:

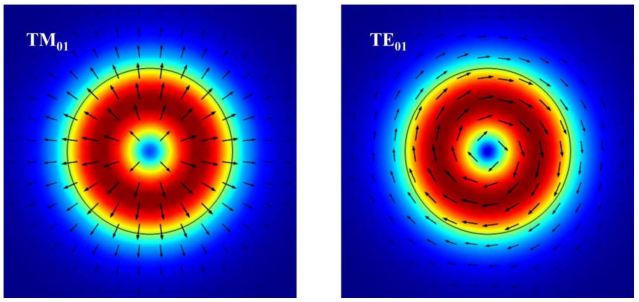

Fig. 7. Polarization and intensity profiles of ultrafast CVBs: (a) radial polarization TM_{01}, (b) angular polarization TE_{01}.

$$E(r,\varphi) = E_0(r)[\cos\ \varphi_0\hat{r} + \sin\ \varphi_0\hat{\varphi}]. \quad (1)$$

φ_0 is the angle between the positive half axis of the Y axis and the electric field line, and the orthogonal TM_{01} mode and TE_{01} mode correspond to Eq. (1) at $\varphi_0 = 0°$ and 90°, respectively. For vector-locked solitons, the vector-locked characteristics and high DOP guarantee the polarization components of vector-locked solitons are partially consistent with those of the TM_{01} mode and TE_{01} mode, which is beneficial to improving the coupling efficiency of the solitons to the TM_{01} mode and TE_{01} mode. On the contrary, the periodical or irregular change of the vector properties of solitons makes it impossible to find the identical vector state in CVBs, so the conversion efficiency of scalar solitons and vector solitons with vectors changing periodically into CVBs will not be improved. However, the improved coupling efficiency of vector-locked solitons leads to nonuniform intensity profiles of CVBs, as shown in Figs. 4(a1) and 4(f1).

3. Conclusion

In conclusion, we investigate the effect of vector dynamics on ultrafast CVBs implementation and innovatively propose a novel technical method to realize femtosecond CVBs based on vector-locked solitons (GVLVSs). The vector-locked solitons are obtained by an all-fiber passively mode-locked laser. Compared with vector-periodically-changed solitons and scalar solitons, the excellent vector-locked characteristics of GVLVSs not only increase the conversion efficiency of solitons to CVBs and the output power of CVBs by 4.1 times and 2.4 times, respectively, but also expand the ultrafast CVBs from the fundamental frequency to harmonic regime for the first time, to the best of our knowledge. The femtosecond CVBs at 1564.72 nm can be tuned from 25 MHz to 198 MHz, corresponding to the fundamental repetition rate to the eighth harmonic order, with the calculated purity of 97.2%. This is the highest repetition rate reported for ultrafast CVBs based on passive mode-locking. This ultrafast CVB based on vector-locked solitons not only opens up their applications in high-repetition rate fields, but also provides a new idea for generation of high-order ultrafast optical vortices.

Acknowledgement

This work was supported by the National Natural Science Foundation of China (NSFC) (Nos. 61805023, 61804013, and 61804014).

References

1. L. Wang, R. M. Nejad, A. Corsi, J. Lin, Y. Messaddeq, L. Rusch, and S. LaRochelle, "Linearly polarized vector modes: enabling MIMO-free mode-division multiplexing," Opt. Express **25**, 11736 (2017).
2. A. Bouhelier, F. Ignatovich, A. Bruyant, C. Huang, G. Colas des Francs, J.-C. Weeber, A. Dereux, G. P. Wiederrecht, and L. Novotny, "Surface plasmon interference excited by tightly focused laser beams," Opt. Lett. **32**, 2535 (2007).
3. M. C. Zhong, L. Gong, D. Li, J. H. Zhou, Z. Q. Wang, and Y. M. Li, "Optical trapping of core-shell magnetic microparticles by cylindrical vector beams," Appl. Phys. Lett. **105**, 181112 (2014).
4. N. A. Chaitanya, S. C. Kumar, G. K. Samanta, and M. Ebrahim-Zadeh, "Ultrafast optical vortex beam generation in the ultraviolet," Opt. Lett. **41**, 2715 (2016).
5. T. Watanabe, Y. Iketaki, T. Omatsu, K. Yamamoto, S. I. Ishiuchi, M. Sakai, and M. Fujii, "Two-color far-field super-resolution microscope using a doughnut beam," Chem. Phys. Lett. **371**, 634 (2003).
6. K. Toyoda, K. Miyamoto, N. Aoki, R. Morita, and T. Omatsu, "Using optical vortex to control the chirality of twisted metal nanostructures," Nano Lett. **12**, 3645 (2012).
7. Y. Song, Z. Wang, C. Wang, K. Panajotov, and H. Zhang, "Recent progress on optical rogue waves in fiberlasers: status, challenges, and perspectives," Adv. Photon. **2**, 024001 (2021).
8. Y. Song, X. Shi, C. Wu, D. Tang, and H. Zhang, "Recent progress of study on optical solitons in fiber lasers," Appl. Phys. Rev. **6**, 021313 (2019).
9. Y. F. Song, L. Li, H. Zhang, D. Y. Shen, D. Y. Tang, and K. P. Loh, " Vector multi-soliton operation and interaction in a graphene mode-locked fiber laser," Opt. Express **21**, 10010 (2013).
10. D. Mao, X. Liu, and H. Lu, "Observation of pulse trapping in a near-zero dispersion regime," Opt. Lett. **37**, 2619 (2012).
11. X. Luo, T. H. Tuan, T. S. Saini, H. P. T. Nguyen, T. Suzuki, and Y. Ohishi, "Group velocity locked vector soliton and polarization rotation vector soliton generation in a highly birefringent fiber laser," Jpn. J. Appl. Phys. **58**, 020910 (2019).
12. Y. Luo, J. Cheng, B. Liu, Q. Sun, L. Li, S. Fu, D. Tang, L. Zhao, and D. Liu, "Group-velocity-locked vector soliton molecules in fiber lasers," Sci. Rep. **7**, 2369 (2017).
13. R. Tao, H. Li, Y. Zhang, P. Yao, L. Xu, C. Gu, and Q. Zhan, "All-fiber mode-locked laser emitting broadband-spectrum cylindrical vector mode," Opt. Laser Technol. **123**, 105945 (2020).
14. Y. Guo, Y. G. Liu, Z. Wang, Z. Wang, and H. Zhang, "All-fiber mode-locked cylindrical vector beam laser using broadband long period grating," Laser Phys. Lett. **15**, 085108 (2018).
15. D. Mao, T. Feng, W. Zhang, H. Lu, Y. Jiang, P. Li, B. Jiang, Z. Sun, and J. Zhao, "Ultrafast all-fiber based cylindrical-vector beam laser," Appl. Phys. Lett. **110**, 021107 (2017).
16. Y. Zhou, J. Lin, X. Zhang, L. Xu, C. Gu, B. Sun, A. Wang, and Q. Zhan, "Self-starting passively mode-locked all fiber laser based on carbon nanotubes with radially polarized emission," Photon. Res. **4**, 327 (2016).
17. H. Wan, J. Wang, Z. Zhang, J. Wang, S. Ruan, and L. Zhang, "Passively mode-locked ytterbium-doped fiber laser with cylindrical vector beam generation based on mode selective coupler," J. Light. Technol. **36**, 3403 (2018).
18. W. Zhang, K. Wei, L. Huang, D. Mao, B. Jiang, F. Gao, G. Zhang, T. Mei, and J. Zhao, "Generation of femtosecond optical vortex pulse in fiber based on an acoustically induced fiber grating," Opt. Express **24**, 19278 (2016).
19. J. Lin, K. Yan, Y. Zhou, L. X. Xu, C. Gu, and Q. W. Zhan, "Tungsten disulphide based all fiber Q-switching cylindrical-vector beam generation," Appl. Phys. Lett. **107**, 191108 (2015).

20. C. Wang, B. Yang, M. Cheng, S. Cheng, J. Liu, J. Xiao, H. Ye, Y. Li, D. Fan, and S. Chen, "Cylindrical vector beam multiplexing for radio-over-fiber communication with dielectric metasurfaces," Opt. Express **28**, 38666 (2020).
21. X. Yi, X. Ling, Z. Zhang, Y. Li, X. Zhou, Y. Liu, S. Chen, H. Luo, and S. Wen, "Generation of cylindrical vector vortex beams by two cascaded metasurfaces," Opt. Express **22**, 17207 (2014).
22. Z. Shen, R. Li, S. Huang, B. Zhang, and Q. Chen, "Generation of needle beams through focusing of azimuthally polarized vortex beams by polarization-insensitive metasurfaces," J. Opt. Soc. Am. B **38**, 1869 (2021).
23. Y. Xu, H. Zhang, Q. Li, X. Zhang, Q. Xu, W. Zhang, C. Hu, X. Zhang, J. Han, and W. Zhang, "Generation of terahertz vector beams using dielectric metasurfaces via spin-decoupled phase control," Nanophotonics. **9**, 3393 (2020).
24. L. Yun, "Generation of vector dissipative and conventional solitons in large normal dispersion regime," Opt. Express **25**, 18751 (2017).
25. B. Sun, A. Wang, L. Xu, C. Gu, Z. Lin, H. Ming, and Q. Zhan, "Low-threshold single wavelength all-fiber laser generating cylindrical vector beams using a few-mode fiber Bragg grating," Opt. Lett. **37**, 464 (2012).